Received: 6 September 2020 | Revised: 27 October 2020 | Accepted: 8 November 2020

DOI: 10.1002/aoc.6108

Applied Organometallic Chemistry WILEY

FULL PAPER

Antimicrobial, computational, and molecular docking studies of Zn (II) and Pd (II) complexes derived from piperidine dithiocarbamate

Ahmed S.M. Al-Janabi[1] | **Mustafa M. Kadhim**[2,3] | **Amenah I.A. Al-Nassiry**[4] | **Tarek A. Yousef**[5,6]

[1]Department of Biochemistry, College of Veterinary Medicine, Tikrit University, Tikrit, Iraq

[2]Department of Chemistry, College of Science, Wasit University, Kut, Iraq

[3]Department of Chemistry, College of Science, Baghdad University, Baghdad, Iraq

[4]Department of Chemistry, College of Education for Pure Science, Tikrit University, Tikrit, Iraq

[5]Chemistry Department, Science College, Imam Mohammad Ibn Saud Islamic University, Riyadh, Saudi Arabia

[6]Toxic and Narcotic Drug, Forensic Medicine Department, Mansoura Laboratory, Medicolegal Organization, Ministry of Justice, Egypt

Correspondence
Ahmed S. M. Al-Janabi, Department of Biochemistry, College of Veterinary Medicine, Tikrit University, Tikrit, Iraq.
Email: dr.ahmed.chem@tu.edu.iq; a_sh200683@yahoo.com

Mixed ligand complexes of Zn (II) and Pd (II) have been prepared from piperidine dithiocarbamate (PipDT) and amine ligand {2,2′-bipyridine (Bipy), 1,10-phenanthroline (Phen), and 3-aminopyridine (3Apy)} to afford complexes of the type [M(κ^1-PipDT)(κ^2-Bipy)] {M^{II}═Zn, Pd} (**1**,**4**), [M(κ^1-PipDT)(κ^2-Phen)] (**2**,**5**), and [M(κ^1-PipDT)(κ^1-3Apy)$_2$] (**3**,**6**). The reaction of equivalent molar of sodium benzisothiazolinate (Nabit) or sodium saccharinate (Nasac) with *cis*-[$PdCl_2(PPh_3)_2$], followed by addition, sodium piperidine dithiocarbamate (NaPipDT) afforded complexes of the type *trans*-[Pd(κ^1-PipDT)(κ^1-N-bit)(PPh_3)$_2$] (**7**) and *trans*-[Pd(κ^1-PipDT)(κ^1-N-sac)(PPh_3)$_2$] (**8**). The obtained complexes were characterized by elemental analysis and spectroscopic techniques. The **PipDT**$^-$ was bonded as monodentate fashion via sulfur atom, whereas the diamine ligands were coordinated as bidentate chelating, while the **3Apy** ligand bonded as monodentate mode through the nitrogen of heterocyclic ring. In complexes (**7**) and (**8**), the **bit**$^-$ and **sac**$^-$ ligand coordinated as monodentate through the nitrogen atom of heterocyclic ring. The antimicrobial activity of the complexes was tested. All the complexes showed moderate to good activity compared with standard antimicrobial. Moreover, the calculations of the density functional theory (DFT) were performed to estimate the thermal parameters, dipole moment, polarizability, and molecular electrostatic potential of the present complexes; in addition, Mulliken atomic charges of the complexes, total electron density (TED), electrostatic surface potential (ESP), lethal concentration (LC_{50}), and docking studies as well as the descriptors of chemical reactivity were studied.

KEYWORDS

antimicrobial, dithiocarbamate, molecular docking, palladium, zinc

1 | INTRODUCTION

Dithiocarbamate compounds ($R_2NCS_2^-$ or $RNHCS_2^-$) are impartial one example of a general class of monoanionic 1,1-dithiolate ligands, which also contains other commonly utilized ligands such as xanthates, carbamates, dithiophosphates (Chart **1**), and many others.[1–6]

The dithiocarbamate synthesis has a large variety, depending on the final product. The traditional method is based on the reaction of a primary or secondary amine

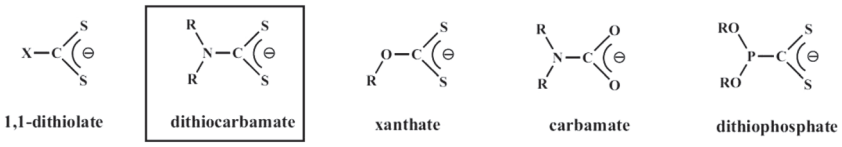

CHART 1 Monoanionic 1,1-dithiolate ligands

with carbon disulfide in the presence of metal or alkaline salt, due to low stability of these acids.[6–22]

Metal complexes of dithiocarbamate ligands have been the subject of current and growing interest because it possesses wide range of medical fields.[1–11] Dithiocarbamate can bond to metal ions in different coordination modes (Chart 2) as (i) monodentate ligands through the sulfur of the CSS^- group (**A**);[10–15] (ii) bidentate chelating fashion through the sulfur atoms, through production of two almost equal M–S bonds. In doing so, it forms a small bite angle (S-M-S), ranging from 65° to 80° being dependent upon the size of the ligand and metal ion (**B**);[7,9,16–38] (iii) bidentate bridging mode through the two sulfur atoms or through the one of the sulfur atom only (**C**);[26,37,39–41] (iv) poly-dentate mode between three center or more (**D**).[28,37,42–44] Metal complexes of dithiocarbamate present a wide range of applications in agricultural science, medicine as antibacterial, anti-fungal, and anti-inflammatory, industry, analytical, and organic chemistry.[1–11]

In the present work, we describe the synthesis, characterization, and biological activity of Zn (II) and Pd (II) mixed ligand complexes of piperidine dithiocarbamate (PipDT) and amine ligands {2,2′-bipyridineine (Bipy), 1,10-phenanthroline (Phen), and 3-aminopyridine (3Apy)}, whereas the treatment of *cis*-$[PdCl_2(PPh_3)_2]$ with sodium benzisothiazolinate (Nabit) or sodium saccharinate (Nasac), followed by addition, sodium piperidine dithiocarbamate (NaPipDT) to give complexes of the type *trans*-$[Pd(\kappa^1\text{-PipDT})(\kappa^1\text{-N-bit})(PPh_3)_2]$ (**7**) and *trans*-$[Pd(\kappa^1\text{-PipDT})(\kappa^1\text{-N-sac})(PPh_3)_2]$ (**8**). Theoretical calculations, particularly Hartree–Fouck (HF) and density functional theory (DFT), have been used to predict the most stable conformation for different compounds and isomers.[45–49]

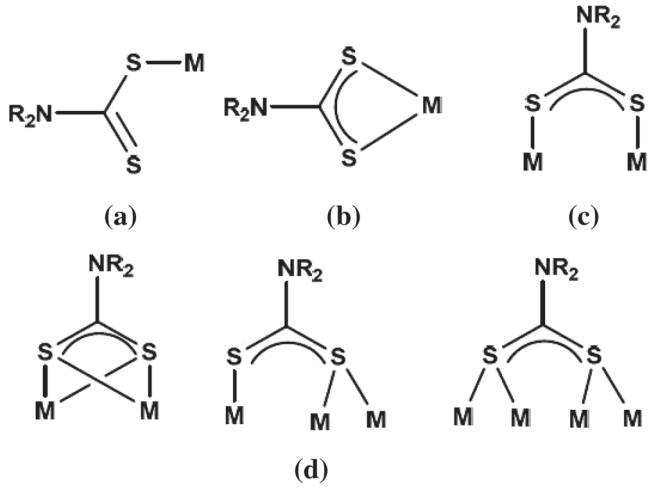

CHART 2 Coordination modes of dithiocarbamate ligands

2 | EXPERIMENTAL

2.1 | Materials and methods

All chemical materials and solvents required were provided from Sigma-Aldrich and used without additional purification. Elemental analysis was determined on a Vario El III elemental analyzer. Infrared spectra were recorded on a Shimadzu Fourier transform infrared (FT-IR) 8400 spectrophotometer using KBr discs in 400- to 4000-cm^{-1} range. ^1H and ^{31}P nuclear magnetic resonance (NMR) spectra were recorded on Bruker 400 apparatus in DMSO-d_6. Molar conductivities were measured by using a digital CD-2005 conductivity meter (10^{-3} M—DMF). The melting point was measured using SMP30 melting point apparatus. The sodium piperidine dithiocarbamate (NaPipDT),[19] $[Zn(\kappa^2\text{-PipDT})_2]$,[19] $[Pd(\kappa^2\text{-PipDT})_2]$,[35] and *cis*-$[PdCl_2(PPh_3)_2]$[50] were prepared by literature methods. The antibacterial activities of the complexes were tested by agar disc diffusion method originally described by Bauer[51] against three bacteria types, *Staphylococcus aureus*, *Staphylococcus pyogenes*, and *Escherichia coli* in (10^{-3} μg/mL of freshly solution in DMSO), also tested against two types of fungi, *Candida albicans* and *Aspergillus niger* at same concentration.

2.2 | Preparation of $[Zn(\kappa^1\text{-PipDT})_2(Bipy)]$ (1)

A solution of 2,2′-bipridyine (Bipy) (0.100 g, 0.64 mmol) in chloroform (10 mL) was added to a suspension of $[Zn(\kappa^2\text{-PipDT})_2]$ (0.247 g, 0.64 mmol) in chloroform (10 mL); the mixture was stirred for 3 h at room temperature, then refluxed for 4 h, and set aside for evaporate slowly. The produced creamy solid was filtered off washed with ethanol and dried under vacuum to afford a creamy powder as $[Zn(\kappa^1\text{-PipDT})_2(Bipy)]$ (**1**).

The following complexes, $[Zn(\kappa^1\text{-PipDT})_2(Phen)]$ **(2)**, $[Zn(\kappa^1\text{-PipDT})_2(3Apy)_2]$ **(3)**, $[Pd(\kappa^1\text{-PipDT})_2(Bipy)]$ (**4**),

[Pd(κ^1-PipDT)$_2$(Phen)] (**5**), and [Pd(κ^1-PipDT)$_2$(3Apy)$_2$], (**6**) were prepared in a similar method.

2.2.1 | [Zn(κ^1-PipDT)$_2$(Bipy)] (1)

Creamy solid. Yield: (0.282 g, 81%). Anal. calc. for $C_{22}H_{28}ZnN_4S_4$: C, 48.74; H, 5.21; N, 10.34. Found: C, 48.96; H, 5.12; N, 10.56%. Molar conductivity in DMF: 8.5 (Ω^{-1} cm^{-1} mol^{-1}). IR (KBr) 3058w, 2973m, 2917w, 1598s, 1505s, 1438s, 1244s, 1163s, 988s, 891s, 672m, 417w, cm^{-1}. ^{1}H NMR (dmso-d^6): δ 1.52(m, 4H, 2CH$_2$-PipDT); 1.97 (m, 8H, 4CH$_2$-PipDT); 4.06 (t, 8H, J_{HH} = 7.8 Hz, 4CH$_2$-PipDT); 7.56 (dd, 2H, J_{HH} = 7.8 Hz, H-Bipy); 7.85 (d, 2H, J_{HH} = 7.6 Hz, H-Bipy); 8.54 (dd, 2H, J_{HH} = 7.6 Hz, H-Bipy); 8.91 (d, 2H, J_{HH} = 8.0 Hz, H-Bipy), ppm. Melting point: 230–233°C.

2.2.2 | [Zn(κ^1-PipDT)$_2$(Phen)] (2)

Off white solid. Yield: (0.319 g, 88%). Anal. calc. for $C_{24}H_{28}ZnN_4S_4$: C, 50.92; H, 4.99; N, 9.90. Found: C, 50.89; H, 5.05; N, 10.13%. Molar conductivity in DMF: 6.0 (Ω^{-1} cm^{-1} mol^{-1}). IR (KBr) 3082w, 2966 m, 2857w, 1573s, 1469s, 1434s, 1271s, 1152s, 995s, 941s, 827s, 664m, 447w, 423w, cm^{-1}. ^{1}H NMR (dmso-d^6): δ 1.68(m, 4H, 2CH$_2$-PipDT); 2.08(m, 8H, 4CH$_2$-PipDT); 4.12(t, 8H, J_{HH} = 8.00 Hz, 4CH$_2$-PipDT); 7.49 (s, 2H, H-Phen); 7.89 (d, 2H, J_{HH} = 8.0 Hz, H-Phen); 8.56 (d, 2H, J_{HH} = 8.0 Hz, H-Phen); 8.98 (t, 2H, J_{HH} = 8.0 Hz, H-Phen), ppm. Melting point: 245°C (decompose).

2.2.3 | [Zn(κ^1-PipDT)$_2$(3Apy)$_2$] (3)

Off white. Yield: (0.176 g, 85%). Anal. Calc. for $C_{22}H_{32}ZnN_6S_4$: C, 46.02; H, 5.62; N, 14.64. Found: C, 45.94; H, 5.81; N, 14.72%. IR (KBr): 3345m, 3,159m, 3058w, 2923m, 2871w, 1587s, 1504s, 1431s, 1266s, 1147s, 1042s, 972s, 657m, 443w cm^{-1}. ^{1}H NMR (DMSO-d_6): δ 1.73 (m, 4H, 2CH$_2$-PipDT); 2.11 (m, 8H, 4CH$_2$-PipDT); 4.08 (t, 8H, J_{HH} = 8.00 Hz, 4CH$_2$-PipDT); 5.56 (bs, 4H, NH$_2$); 6.78 (s, 2H, H-3Apy); 7.43 (dd, 2H, J_{HH} = 7.6 Hz, H-3Apy); 7.88 (d, 2H, J_{HH} = 7.6 Hz, H-3Apy); 8.03(d, 2H, J_{HH} = 7.4 Hz, H-3Apy). Melting point: 159–162°C.

2.2.4 | [Pd(κ^1-PipDT)$_2$(Bipy)] (4)

Creamy solid. Yield: (0.342 g, 92%). Anal. calc. for $C_{22}H_{28}PdN_4S_4$: C, 45.31; H, 4.84; N, 9.61. Found: C, 45.20; H, 4.61; N, 9.88%. Molar conductivity in DMF: 8.5 (Ω^{-1} cm^{-1} mol^{-1}). IR (KBr) 3058w, 2973m, 2917w, 1598s, 1505s, 1438s, 1244s, 1163s, 988s, 891s, 672m, 417w, cm^{-1}. 1.69 (m, 4H, 2CH$_2$-PipDT); 2.01 (m, 8H, 4CH$_2$-PipDT); 4.08 (t, 8H, J_{HH} = 7.8 Hz, 4CH$_2$-PipDT); 7.46 (dd, 2H, J_{HH} = 7.8 Hz, H-Bipy); 7.69 (t, 2H, J_{HH} = 7.6 Hz, H-Bipy); 8.40 (d, 2H, J_{HH} = 7.6 Hz, H-Bipy); 8.69 (d, 2H, J_{HH} = 8.0 Hz, H-Bipy), ppm. Melting point: 260°C (decompose).

2.2.5 | [Pd(κ^1-PipDT)$_2$(Phen)] (5)

Off white solid. Yield: (0.289 g, 75%). Anal. calc. for $C_{24}H_{28}PdN_4S_4$: C, 47.48; H, 4.65; N, 9.23. Found: C, 47.76; H, 4.81; N, 9.49%. Molar conductivity in DMF: 6.0 (Ω^{-1} cm^{-1} mol^{-1}). IR (KBr) 3084w, 2966m, 2858w, 1573s, 1512s, 1434s, 1271s, 1152s, 993s, 908s, 662m, 423w, cm^{-1}. 1.58 (m, 4H, 2CH$_2$-PipDT); 1.99 (m, 8H, 4CH$_2$-PipDT); 4.05 (t, 8H, J_{HH} = 8.00 Hz, 4CH$_2$-PipDT); 7.49 (s, 2H, H-Phen); 7.89 (d, 2H, J_{HH} = 8.0 Hz, H-Phen); 8.56 (d, 2H, J_{HH} = 8.0 Hz, H-Phen); 8.98 (t, 2H, J_{HH} = 8.0 Hz, H-Phen), ppm. Melting point: 285°C (decompose).

2.2.6 | [Pd(κ^1-PipDT)$_2$(3Apy)$_2$] (6)

Light brown powder. Yield: (0.329 g, 84%). Anal. Calc. for $C_{22}H_{32}PdN_6S_4$: C, 42.95; H, 5.24; N, 13.66. Found: C, 42.75; H, 5.11; N, 13.72%. IR (KBr): 3295m, 3163m, 3058w, 2923m, 2871w, 1593s, 1504s, 1431s, 1266s, 1147s, 1063s, 956s, 657m, 443w cm^{-1}. ^{1}H NMR (DMSO-d_6): δ 1.68 (m, 4H, 2CH$_2$-PipDT); 2.09 (m, 8H, 4CH$_2$-PipDT); 4.12 (t, 8H, J_{HH} = 8.00 Hz, 4CH$_2$-PipDT); 6.02 (bs, 4H, NH$_2$); 6.92 (s, 2H, H-3Apy); 7.39 (t, 2H, J_{HH} = 7.8 Hz, H-3Apy); 7.72 (d, 2H, J_{HH} = 7.6 Hz, H-3Apy); 7.96 (d, 2H, J_{HH} = 7.8 Hz, H-3Apy). 240°C (decompose).

2.3 | Preparation of *trans*-[Pd(κ^1-PipDT)(κ^1-N-bit)(PPh$_3$)$_2$] (7)

A hot solution of sodium benzisothiazolinate (Nabit) (0.050 g, 0.289 mmol) in ethanol (10 mL) was added to a yellow solution of *trans*-[PdCl$_2$(PPh$_3$)$_2$] (0.202 g,0.289 mmol) in dichloromethane (10 mL); the mixture was stirred for 2 h then a solution of NaPipDT (0.053 g, 0.289 mmol) in ethanol (5 mL) was added. The mixture was refluxed for 4 h, to give light brown solution. The produced brown solution was filtered off and set aside to evaporate slowly. The brown solid formed was filtered off washed with hot ethanol and dried under vacuum. The *trans*-[Pd(κ^1-PipDT)(κ^1-*N*-sac)(PPh$_3$)$_2$] (**8**) complex was prepared in a similar method.

2.3.1 | *trans*-[Pd(κ^1-PipDT)(κ^1-*N*-bit)(PPh_3)$_2$] (7)

Yellowish brown powder. Yield: (0.239 g, 88%). Anal. calc. for $C_{49}H_{44}PdN_2OP_2S_3$: C, 62.51; H, 4.71; N, 2.98. Found: C, 62.51; H, 4.71; N, 2.98%. Molar conductivity in DMF: 4.30 (Ω^{-1} cm^{-1} mol^{-1}). IR (KBr) 3072w, 2942w, 1618s, 1579s, 1520s, 1453s, 1436s, 1276s, 1123s, 1013m, 953m, 498s cm^{-1}. ^{1}H NMR ($CDCl_3$): δ 1.56 (m, 4H, 2CH_2-PipDT); 1.98 (dd, 8H, J_{HH} = 7.4 Hz, 4CH_2-PipDT); 3.98 (t, 8H, J_{HH} = 7.6 Hz, 4CH_2-PipDT); 7.39–7.78 (m, 34H, H-phenyl (bit + 2PPh_3) ppm. Melting point: 231–233°C.

2.3.2 | *trans*-[Pd(κ^1-PipDT)(κ^1-*N*-sac)(PPh_3)$_2$] (8)

Brown powder. Yield: (0.217 g, 77%). Anal. calc. for $C_{49}H_{44}PdN_2O_3P_2S_3$: C, 60.46; H, 4.56; N, 2.88. Found: C, 60.71; H, 4.42; N, 3.14%. Molar conductivity in DMF: 4.30 (Ω^{-1} cm^{-1} mol^{-1}). IR (KBr) 3035w, 2923w, 1648s, 1547s, 1512s, 1451s, 1434s, 1244s, 1153s, 997s, 936m, 487m cm^{-1}. ^{1}H NMR (DMSO-d_6): δ 1.62 (m, 4H, 2CH_2-PipDT); 2.02 (dd, 8H, J_{HH} = 7.4 Hz, 4CH_2-PipDT); 4.10 (t, 8H, J_{HH} = 7.6 Hz, 4CH_2-PipDT); 7.23–7.86 (m, 34H, H-phenyl (sac + 2PPh_3)) ppm. Melting point: 231°C (decompose).

2.4 | Computational methods

Research Collaboratory for Structural Bioinformatics (RCSB) used to download the protein structure (3wze).[52] The protein and complexes structures were processed to a format recognized by the AutoDock tools (ADT) (*.pdbqt files) by adding all hydrogen atoms, Gasteiger charges, and merging the polar hydrogen atoms by Molecular Graphic Laboratory (MGL) tools program.[53] The root for the molecule identify by the Auto-dock automatically. The atoms' specific affinity maps for all ligand atom types, electrostatic, and desolation potentials were computed with the help of Auto grid (version 4.2.6).[54] The DFT calculations were performed with the hybrid DFT functional B3LYP, as implemented by the Gaussian 09 program package. This function utilizes the Becke three-parameter exchange functional (B3), combined with the correlation functional of Lee, Yang, and Parr (LYP). The Pd and Zn atoms were described by Stuttgart–Dresden effective core potentials (ECP) and an SDD basis set, while the 6-31G(d′) basis set was employed for the remaining atoms.[55] Total electron density (TED) and electrostatic surface potential (ESP) maps were calculated by DFT/STO-3G method.[56]

3 | RESULTS AND DISCUSSION

3.1 | Synthesis and characterization [M(κ^1-PipDT)$_2$(κ^2-Bipy)] {M^{II}=Zn, Pd} (1,4) and [M(κ^1-PipDT)$_2$(κ^2-Phen)] (2,5)

The reactions of complexes (**1**) or (**2**) with equimolar amounts of diamine ligands (Bipy or Phen) afforded complexes of the type [M(κ^1-PipDT)$_2$(κ^2-Bipy)] {M^{II} = Zn, Pd} (**1**,**4**) and [M(κ^1-PipDT)$_2$(κ^2-Phen)] (**2**,**5**) (Scheme 1). The dithiocarbamate ligand was coordinated through the sulfur atom as monodentate fashion, whereas the diamine ligand was bonded as bidentate chelating ligand through the nitrogen atoms. The prepared complexes are soluble in DMSO and DMF and partially soluble in warm $CHCl_3$ or CH_2Cl_2; the complexes were investigated by using elemental analysis, molar conductivity, ^{1}H-NMR, and IR techniques, and data are given in Section 2. All attempts to get crystals suitable for X-ray diffraction studies were unsuccessful.

The IR spectra of the complexes (Figure S1) displayed a strong bands within the 1602- to 1583-cm^{-1} range, assigned to the υ(C═N) of the diamine ligands. These were shifted to lower frequencies of that in the free ligands; this means that coordination of the amine took place through the endocyclic nitrogen atoms.[20,25,32,33,57] The PipDT ligand displayed two distinguishing bands within 941–972 and 995–1063 cm^{-1} due to ν(C–S) and ν(C═S), respectively; the dithiocarbamate ligand displayed two characteristic bands compared with [M(κ^2-PipDT)$_2$] {M^{II}=Zn, Pd} (showed one band) and indicated that the PipDT bonded as monodentate model to the M (II) ion through the sulfur atom.[7,10,58] The spectra also diplayed υ(M–N) within the 443- to 496-cm^{-1} range[50,59] and υ(M–S) bond within the 418- to 455-cm^{-1} range.[50,59]

^{1}H-NMR spectra of [M(κ^1-PipDT)$_2$(κ^2-Bipy)] {M^{II}=Zn, Pd} (**1**,**4**) and [M(κ^1-PipDT)$_2$(κ^2-Phen)] (**2**,**5**) complexes (Figure 1) clearly display the protons belong to the Bipy or Phen and $PipDT^-$ ligands. The ^{1}H NMR specrta showed the protons of $PipDT^-$ ligand as three unglued peaks within 1.47–1.69, 1.82–2.08, and 4.02–4.12 ppm, due to the methylene groups. Whereas the protons of phenyl rings in diamine ligands displayed as a resolved peak in the aromatic region, and the integrations under signals are in agreement with the number of protons. All these peaks are listed in Section 2.

3.2 | Synthesis and characterization [M(κ^1-PipDT)$_2$(κ^1-Apy)$_2$] {M^{II}=Zn, Pd} (3,6)

Two moles of 3-aminopyridine ligand was reacted with one mole of complex (**1**) or (**2**) to give complexes of the

SCHEME 1 Preparation of complexes **1**, **2**, **4**, and **5**

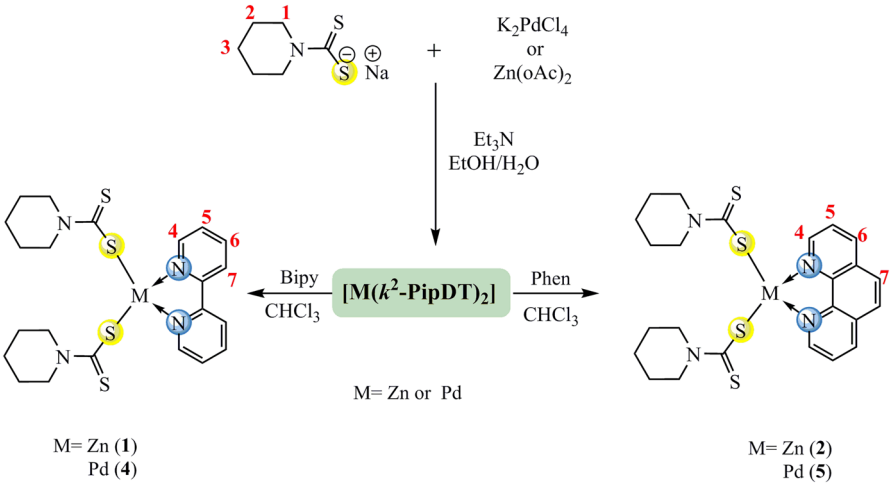

FIGURE 1 ^{1}H nuclear magnetic resonance (NMR) spectrum of complex [Pd(κ^1-PipDT)$_2$(κ^2-Bipy)$_2$] (**1**)

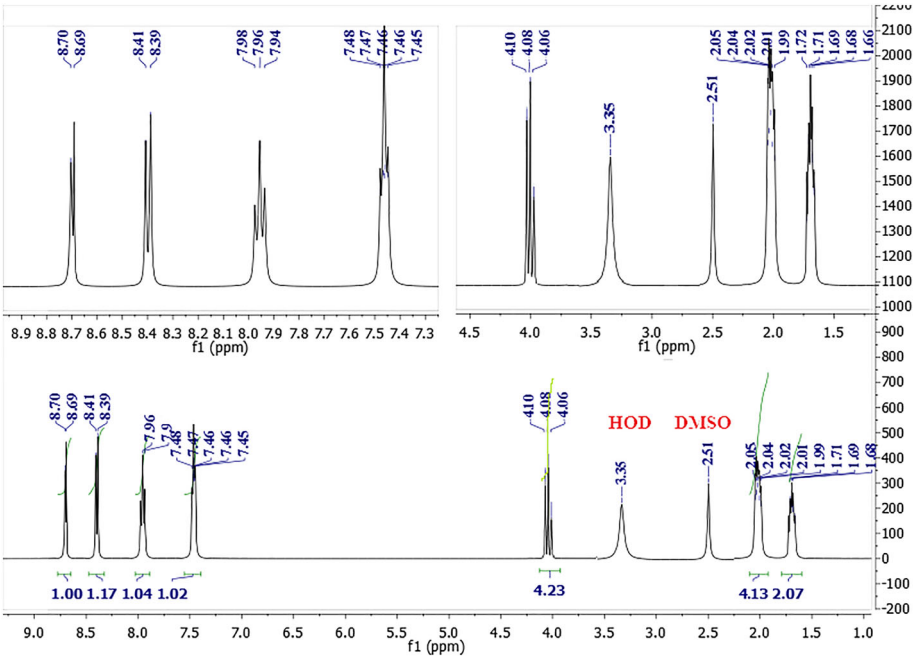

type [M(κ^1-PipDT)$_2$(κ^1-3Apy)$_2$] {M^{II}=Zn, Pd} (**3**,**6**) (Scheme 2). The 3Apy ligand was bonded as monodentate model through the nitrogen of heterocyclic ring. Also the PipDT$^-$ ligand was coordinated as monodentate fashion through sulfur atom of CSS$^-$ group. The complexes were investigated by using elemental analysis, molar conductivity, ^{1}H-NMR, and IR techniques. Data are given in Section 2. All attempts to get crystals suitable for X-ray diffraction studies were unsuccessful.

Selected IR bands of the complexes (**3**) and (**6**) are listed in Section 2. The IR spectra displayed the υ(C=N) at 1587 and 1593 cm^{-1} for the **3** and **6**, respectively; this band was shifted to lower frequency compared with the free (3Apy) ligand, indicating that the coordination occurred through the endocyclic nitrogen atom.[16,23,59]

SCHEME 2 Preparation of complexes **3** and **6**

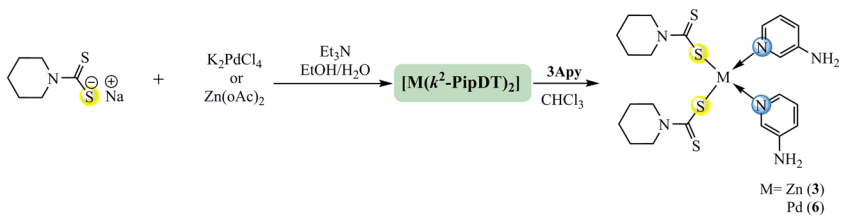

The asymmetric stretching of the NH_2 group observed as sharp to medium intensity bands at 3345 and 3295 cm^{-1}, while the symmetric stretching appeared at 3159 and 3163 cm^{-1} for the complexes (**3**) and (**6**), respectively. This band shifts slightly to higher wave number side relative to the free ligands indicating a noncoordination of the NH_2 group.[57,60] The PipDT ligand displayed two distinguishing bands within 956–972 and 1042–1063 cm^{-1} due to ν(C–S) and ν(C═S), respectively; the appeared two characteristic bands compared with [M(κ^2-PipDT)$_2$] {M^{II}═Zn, Pd} (showed one band) indicated that the PipDT bonded as monodentate model to the M (II) ion through the sulfur atom.[7,10,58]

In the ^{1}H NMR spectra were particularly informative for the protons of $PipDT^-$ and 3-aminpyridine ligands. The protons of the heterocyclic ring of the **3Apy** ligand displayed as four separated peaks in the aromatic range within δ (6.78–8.03 ppm for the complexes (**3**) and (**6**). Whereas the protons of the NH_2 group for 3-aminopyridine displayed a broad singlet at δ 5.56 and 6.02 ppm. The spectra also appeared the protons of the dithiocarbamate ligand as three unglued peaks within (1.68–1.73) ppm, (2.09–2.11) ppm and (4.08–4.12) ppm. Integration values under each signal indicated that two of each of piperidine dithiocarbamate and 3-aminopyrdine are incorporated in each of the prepared complexes.

3.3 | Synthesis and characterization *trans*-[Pd(κ^1-PipDT)(κ^1-N-bit)(PPh_3)$_2$] (7) and *trans*-[Pd(κ^1-PipDT)(κ^1-N-sac)(PPh_3)$_2$] (8)

Reaction of equimolar amount of *cis*-[$PdCl_2(PPh_3)_2$] with sodium benzisothiazolinate (Nabit) or sodium saccharinate (Nasac) followed by addition ethanolic solution of sodium piperidine dithiocarbamate ligand led to formation new products of (**7**) and (**8**) in good yield 88% and 77%, respectively (Scheme 3). The prepared complexes were characterized by using spectroscopic and analytical technical. All attempts to generate crystals suitable for X-ray diffraction studies were unsuccessful. The molar conductivity value referred the complexes (**7**) and (**8**) are nonelectrolyte.

The ^{31}P-{^{1}H} NMR spectra of (**7**) and (**8**) showed a singlet peak at δ P = 29.93 and 30.02 ppm, respectively (Figure 2), indicating the presence of a single products for each and the phosphorus atoms are equivalents.

The ^{1}H-{^{31}P} NMR spectra of (**7**) and (**8**) clearly showed the protons of $PipDT^-$ ligand as three peaks within δ 1.56–1.62, 1.98–2.02, and 3.98–4.10 ppm due to methylene groups. Whereas, the protons of phenyl rings in PPh_3 and sac^- ligands displayed as unresolved within δ 7.39- to 7.78- and 7.23- to 7.86-ppm range for complexes (**7**) and (**8**), respectively. Integration values under each signal indicated that one of each of piperidine dithiocarbamate, saccharinate ligand, and two Ph_3P is incorporated in each of the prepared complexes.

IR spectra of the complexes (**7**) and (**8**) showed the ν(C═O) of the sac^- and bit^- ligands at 1648 and 1618 cm^{-1}, which slightly shifted compared with that of the free saccharinate ligand, indicating that the carbonyl group does not participate in the coordination to metal ions.[61,62] The υ(C–N) band displayed at 1579 and 1547 cm^{-1}; this band was shifted to low frequency region compared with that of the free ligands; this is in agreement with coordination of the sac^- and bit^- ligands with the metal ions occurred through the nitrogen of heterocyclic ring.[62,63] The dithiocarbamate showed two diagnostic bands in the IR spectra, at 936 and 959 and 997 and 1013 cm^{-1} corresponding to ν(C–S) and ν(C═S), respectively; the appeared two characteristic bands compared with [M(κ^2-PipDT)$_2$] {M^{II}═Zn, Pd} (showed one band) indicated that the dithiocarbamate coordinates as monodentate fashion to the Pd (II) ion through the sulfur atom.[7,10,58]

3.4 | Antimicrobial activity

Antimicrobial activity of the sodium piperidine dithiocarbamate ligand and their complexes are listed in Table 1 and summarized in Figure 3**.** The data were obtained against three types of the pathogen bacteria (*E. coli*, *S. aureus*, and *S. pyogenes*) and two fungi types (*C. albicans and A. niger*) in 10^{-3} μg/mL. The standard error for the experiment was ±0.03%, and the experiments were repeated three times at same conditions. The diameter of the inhibitory zone (DIZ) was

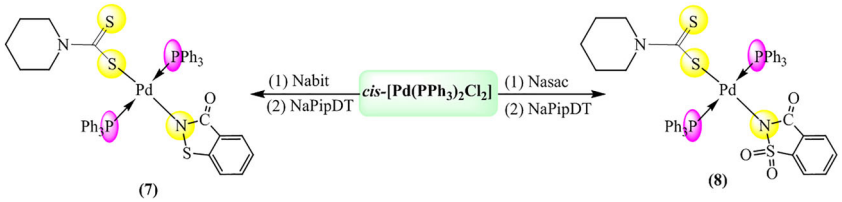

SCHEME 3 Preparation of complexes (**7**) and (**8**)

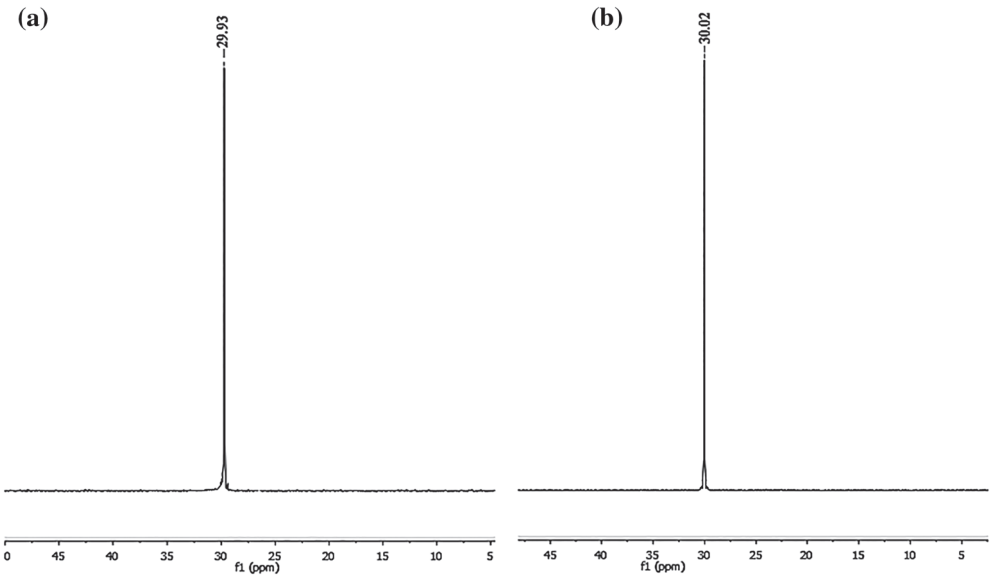

FIGURE 2 The ^{31}P-{^{1}H} nuclear magnetic resonance (NMR) spectra of the (a) complex (**7**) and (b) complex (**8**)

TABLE 1 Results of antimicrobial activities of the compounds in (mm)

	Dimeter inhibition zone (DIZ) in (mm)				
	Bacteria			Fungi	
Compounds	*Escherichia Coli*	*Staphylococcus aureus*	*Pseudomonas aeruginosa*	*Candida albicans*	*Aspergillus niger*
NaPipDT	**8**	**8**	**11**	**7**	**9**
1	**12**	**16**	**14**	**11**	**10**
3	**19**	**17**	**18**	**16**	**12**
4	**12**	**11**	**12**	**14**	**10**
6	**17**	**18**	**16**	**13**	**16**
7	**20**	**20**	**14**	**18**	**15**
8	**24**	**22**	**20**	**22**	**19**
Streptomycin	**23**	**20**	**25**	**NS**	**NS**
Fluconazole	**NS**	**NS**	**NS**	**21**	**23**

Note: Streptomycin: positive control for antibacterial screening; fluconazole: positive control for antifungal screening; NS denotes not screened.

compared with that of streptomycin (as control positive of anti-bacteria) and fluconazole (as control positive of anti-fungi), which is the positive control and used DMSO as negative control. The complexes displayed good activity against the pathogen bacteria. Following results were achieved from the obtained data:

1- The complexes displayed high activity more than free sodium piperidine dithiocarbamate ligand.
2- Biological activities of the compounds were in the order of the following:

8 > 7 > 3 > 6 > 4 > 1 > NaPipDT.

1- The size of a complex could be considered a factor that affects its permeability through the microbial cell wall.[6,63] Arranging the complexes in order of increasing molecular weight gives as follows:

8 > 7 > 6 > 4 > 3 > 1 > NaPipDT.

2- Complexes **8** and **7** showed the highest anti-microbial activity than the other complexes and free ligand. These complexes have two phosphorus atoms with one atom of nitrogen and sulfur around the palladium; we assume that increased might be responsible for the anti-microbial activity, and the benzisothiazolinate (bit^-) or saccharinate (sac^-) has a

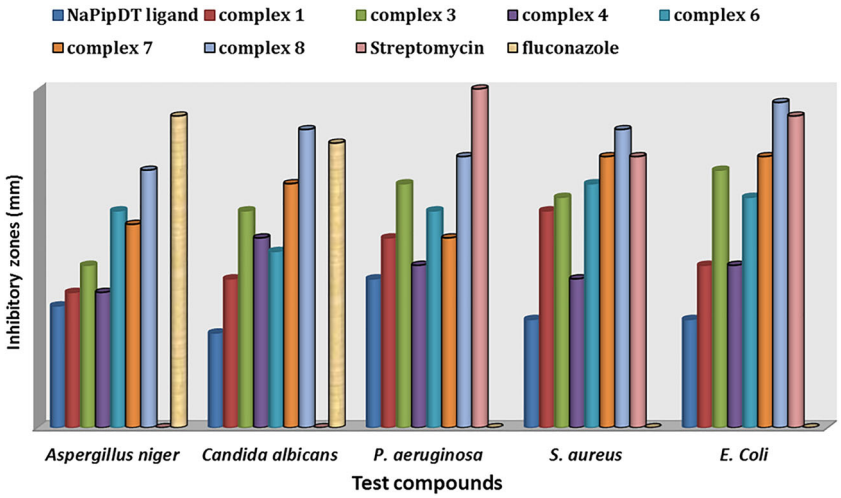

FIGURE 3 A histogram representation of the antimicrobial results of the complexes

heterocyclic ring with C═O, CNS, and SO_2 groups; these act to increase the activity.[64,65]

3- The complex **8** showed greater antibacterial activity compared with streptomycin against *E. coli* and *S. aureus*, also showed greater antifungal activity compared with fluconazole against *C. albicans*.

Their activity of prepared complexes may be referring to many factors:

1- Structure of starting materials such as saccharinate and benzisothiazolinate are good examples of hetero-aromatic organic compounds have biological properties.
2- Chelating effect: The significant activity of metal complexes in inhibiting ability due to incorporation of metal ions increases the inhibition of cell growth.[64–66]
3- Effect of molecular weight: The molecular weight plays a major role in interaction of materials with biological system.

Although, the careful mechanism of biological activity of our compounds is not fully understood biochemically; style of action of biological agents may include any of the following mechanism:

i. Interference with the cell membrane of bacteria or fungi.
ii. Deactivate various cellular enzymes, which play a vital role in different metabolic pathways of these microorganisms.

iii. Formation of hydrogen bond between the function groups with the active site of cell constituents, producing in interference with the normal cell action.[64–66]

3.5 | Theoretical studies

3.5.1 | DFT calculations studies

In this part of this chapter, we propose to give the bases for the understanding of the key concepts of DFT, which provides access to a large number of properties. As it cannot be exhaustive, the emphasis will be placed on the theoretical foundations and the inevitable limits of this theory.

We have analyzed, using DFT, with the aim of evaluating the donor or electron acceptor capacities of these ligands, as well as the analysis of its stability. Likewise, the nature of the metal–ligand and metal–metal bonds of the neutral species will be analyzed as a function of the nature of the metal and of the donor or acceptor capacities of the auxiliary ligand linked to the metal atom.

The theoretical DFT calculations were performed in gas phase by DFT method at B3LYP 6-311G (d,p) basis set. The estimated DFT calculations for electronic energy, heat capacity, entropy (S), thermal energy, polarizability, and dipole moment for **1–8** are summarized in Table 2.

The DFT estimated data revealed that the dipole moment of the complexes under investigation is in the order: $[Zn(\kappa^2\text{-PipDT})_2]$ < **7** < **5** < **1** < $[Pd(\kappa^2\text{-PipDT})_2]$ < **4** < **8** < **6** < **3** < **2**. The high dipole moment **2**, **3**, **4**, and **8** could illustrate their binding pose within a specific target protein and their results of the predicted binding affinity that will be discussed in the following molecular docking part. The polarizability of the materials depends on how the susceptibility of molecular system electron cloud be accepted by approaching of a charge. Moreover, it depends on the complexity of the compounds as well as the size of the molecular structure. Molecules of the large size are more polarizable compounds. It is worth noting that the $[Pd(\kappa^2\text{-PipDT})_2]$ is the smallest in size and has the least polarizability

(218.93 a.u.); however, [Zn(κ^2-PipDT)$_2$] of the highest complexity is predicted to have the highest polarizability (617.48 a.u.).

3.5.2 | Mulliken atomic charges

Assessment of Mulliken atomic charges in the hypothetical estimation process of the molecular structure exhibits considerable responsibility. The distribution of the all complexes charge has been clarified (Table S1). The positive charges of most C, Pd, and Zn atoms were due to their ability to accept them, whereas the negative values of most S, N, and O atoms were due to their ability to give.

3.5.3 | Chemical reactivity descriptors

The most essential orbitals to describe the compound's optical properties and chemical and biological activity of the chemical species are the highest occupied frontier MO's and the lowest unoccupied MO's (highest occupied molecular orbital [HOMO] and lowest unoccupied molecular orbital [LUMO]). The higher value of a molecule's HOMO implies that it acts as a "Lewis Base" or may be oxidation and has the potential to donate electrons to a convenient acceptor molecule with low energy (or empty molecular orbitals), while the higher value of a molecule's lowest unoccupied molecular orbital LUMO implies that it acts as a "Lewis Acid" or is capable of reducing and absorbing electrons from convenient donor molecules.

In our study, the results show that the inhibition and hindrance of protein activity of building complexes complex **2**, **4**, [Zn(κ^2-PipDT)$_2$], **5**, and **1** is higher compared with other complexes with the highest occupied MO (HOMO) and E energy indicating the capacity to donate electrons and building complex stability, respectively, inversely to other complexes.

Recently, many reports showed that the Frontier Orbital Theory in Organic Reactivity (FMOs) have to be taken into consideration in investigation of the structure activity relationships.[67–69] The FMOs theory showed that the energy level of the HOMO and the LUMO is the most significant aspects that impact the bioactivities of small structural drugs. Mainly, HOMOs offer electrons; however, the LUMOs accept electrons. Obviously, the level of energy of HOMOs is different for all studied compounds. [Zn(κ_2-PipDT)$_2$] showed the most lying HOMO than the other compounds, and consequently, it could be a better electron donor drug. Interestingly, [Zn(κ_2-PipDT)$_2$] and **2** of the largest energy gap $\Delta E = 1.64$ and 1.20 eV, respectively, there are several hydrophilic interactions that could facilitate the binding with the receptors. This suggests that such hydrophilic interactions considerably impact the binding affinity of such small drugs to the receptors. The HOMO of a certain drug and the LUMO with the adjacent residues could share the orbital interactions during the binding process.

Calculations, such as the energy of the highest occupied molecular orbital (EHOMO) and energy of the lowest unoccupied molecular orbital (ELUMO), obtain quantium chemical parameters of organic compounds. Additional parameters, such as separation energies (ΔE), absolute electronegativities (ν), chemical potentials (Pi),

TABLE 2 Electronic energy (Hartree/Particle), heat capacity (Cv), entropy (S) (cal/mol-Kelvin), thermal energy, polarizability **α** (a.u.), and dipole moment (Debye) of [Zn(κ^2-PipDT)$_2$], [Pd(κ^2-PipDT)$_2$], and **1–8** complexes

Compounds	Electronic energy	Total dipole moment	Polarizability (α)	E (thermal)	Heat capacity (Cv)	Entropy (S)
[Zn(κ^2-PipDT)$_2$]	−7846.63	3.31	617.48	439.06	122.88	196.05
[Pd(κ^2-PipDT)$_2$]	−7069.78	8.76	218.93	228.98	60.84	126.83
1	−4412.43	8.36	298.76	329.99	81.57	142.69
2	−4487.56	14.82	313.09	339.47	88.17	153.76
3	−4523.25	12.99	304.11	371.41	90.49	157.78
4	−7558.09	10.05	377.16	329.42	80.27	144.52
5	−7633.05	7.62	380.36	330.18	82.18	143.29
6	−7668.55	12.02	267.63	362.29	86.04	150.16
7	−8981.71	6.54	566.39	574.29	135.50	188.91
8	−8832.96	10.49	565.61	569.22	132.34	190.92

TABLE 3 Calculated EHOMO, ELUMO, energy band gap (EH–EL), chemical potential (μ), electronegativity (χ), global hardness (η), global softness (S), global electrophilicity index (ω), and softness (σ) for [Zn(κ^2-PipDT)$_2$], [Pd(κ^2-PipDT)$_2$], and **1–8** complexes

Compounds	EH/eV	EL/eV	(EL–EH)/Ev	χ/eV	μ/eV	η/eV	S/eV^{-1}	ω/eV	σ/eV^{-1}
[Zn(κ^2-PipDT)$_2$]	1.66	2.27	0.61	−1.96	1.96	0.31	0.15	6.31	1.64
[Pd(κ^2-PipDT)$_2$]	0.97	2.44	1.47	−1.70	1.70	0.74	0.37	1.97	0.68
1	−4.32	−2.81	1.51	3.56	−3.56	0.75	0.38	8.43	0.66
2	−0.97	−0.14	0.83	0.56	−0.56	0.42	0.21	0.37	1.20
3	−0.05	1.59	1.63	−0.77	0.77	0.82	0.41	0.36	0.61
4	−0.68	0.44	1.11	0.12	−0.12	0.56	0.28	0.01	0.89
5	−0.62	0.52	1.14	0.05	−0.05	0.57	0.29	0.001	0.88
6	−0.77	0.33	1.10	0.22	−0.22	0.55	0.28	0.04	0.91
7	−0.55	0.87	1.41	−0.16	0.16	0.71	0.35	0.02	0.71
8	−0.45	0.99	1.44	−0.27	0.27	0.72	0.36	0.05	0.69

Abbreviations: EHOMO, energy of the highest occupied molecular orbital; ELUMO, energy of the lowest unoccupied molecular orbital.

absolute hardness (g), absolute softness (r), global electrophilicity (x), and global and softness (S), were calculated by Equations (1)–(5) (Table 3).[70–72]

$$\chi = -1/2\,(E_{\mathrm{LUMO}} + E_{\mathrm{HOMO}}), \quad (1)$$

$$\mu = -\chi = 1/2\,(E_{\mathrm{LUMO}} + E_{\mathrm{HOMO}}), \quad (2)$$

$$\eta = 1/2\,(E_{\mathrm{LUMO}} - E_{\mathrm{HOMO}}), \quad (3)$$

$$S = 1/2\eta, \quad (4)$$

$$\omega = \mu^2/2\eta. \quad (5)$$

The inverse value of the global hardness is designed as the softness (σ) as follows:

$$\sigma = 1/\eta. \quad (6)$$

3.5.4 | Complexes interactions

ESP is the direct interactions of complexes onto the protein functional groups. The present atoms and parts of the complexes are not active in the linkage with protein structure. There is high electron density (red color), low electron density (blue color), and neutral by green color according to TED[73] as shown in Figure S2. Complex **9** is a good inhibition according to docking results in coming parts so the TED and ESP are shown in Figure 4 (for complexes **2**, **4**, **7**, and **8)**. The palladium elements in all complexes have a high electron density. Other than that, the zinc complexes electron density focused on oxygen atoms.

3.5.5 | Lethal concentration method (LC_{50})

LC_{50} is the maximum concentration anoxic of the complexes studied that can be used in human body. HF/3–11 method is used to predict their values of LC_{50}. Equation 7 is used to suggest the values.

$$\mathrm{HF-LogLC_{50}} = 38.00 - 1.13S_{\mathrm{tr}} + 1.38\times10^{-3}\,\omega\,\mathrm{H} - 2.22\times10^{-3}\,\omega\,\mathrm{L} - 0.36I_A\ldots\ldots, \quad (7)$$

where S_{tr} = translational entropy, ω = vibrational wavenumber, and I_A = principal moment of inertia.[74] The heights value complex number 1 (84.8×10^{-10} mol/L) and the lowest value complex 6 (0.11×10^{-10} mol/L) Table 4. The results indicate to the high concentrations could use in human body of the complexes.

3.6 | Docking results

The complexes mentioned were suggested as anticancer by blocking vascular endothelial growth factor receptor

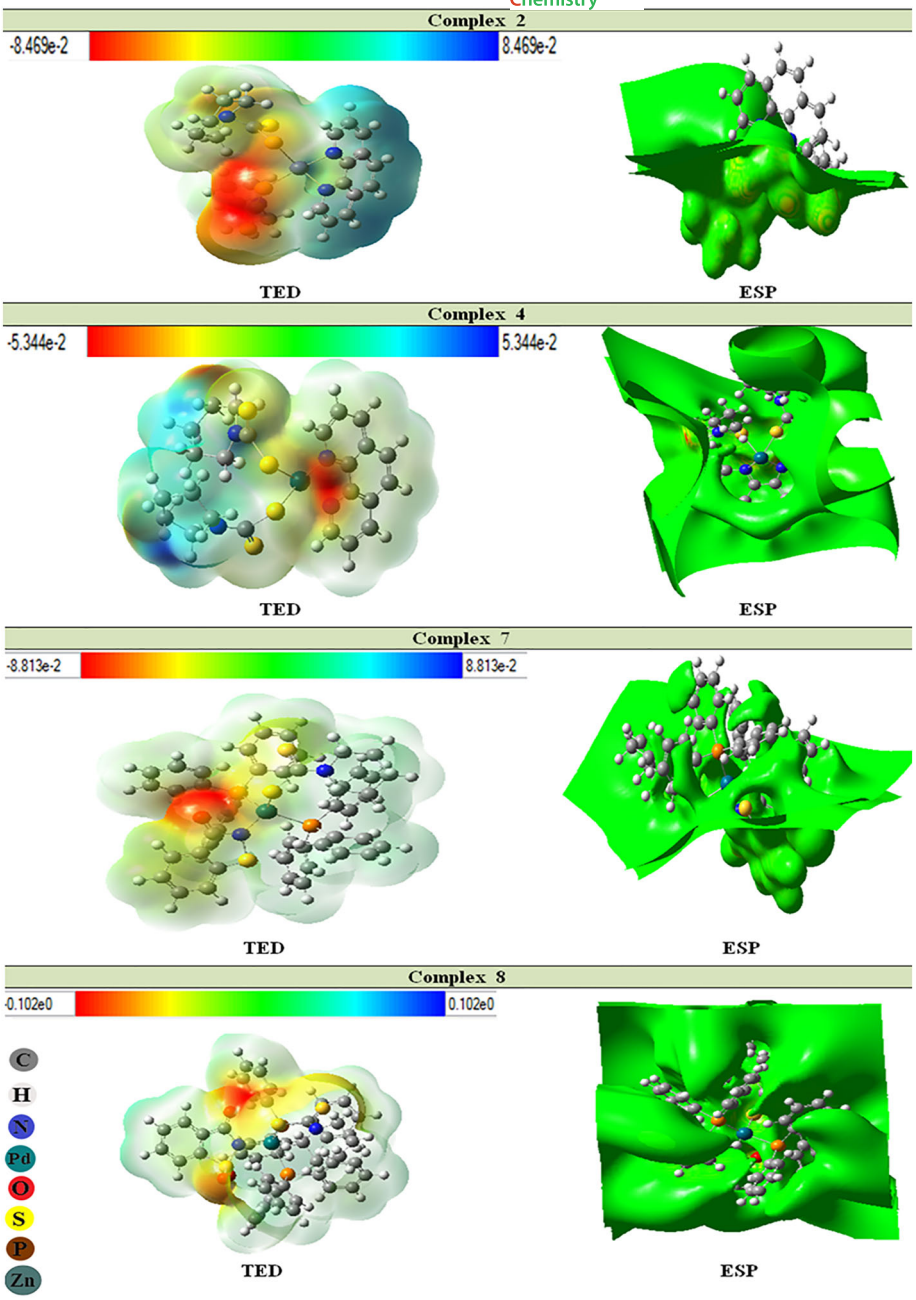

FIGURE 4 Total electron density (TED) and electrostatic surface potential (ESP) of complexes **2**, **4**, **7**, and **8**

TABLE 4 LC_{50} suggested method parameters

Complex	S_{tr}	I_A	ωH	ωL	LC_{50} (mol/L)
[Zn(κ^2-PipDT)$_2$]	45.802	0.99999	2973.64	26.38	84.8×10^{-10}
[Pd(κ^2-PipDT)$_2$]	44.052	0.99999	2977.53	34.60	7.82×10^{-10}
1	44.745	0.99991	3114.91	58.07	0.17×10^{-10}
2	44.875	0.99981	3098.55	27.66	0.13×10^{-10}
3	44.917	0.9996	3287.4	32.20	0.22×10^{-10}
4	44.968	0.99943	3118.35	27.12	0.11×10^{-10}
5	45.089	0.99999	3093.22	75.40	6.17×10^{-10}
6	45.128	0.9954	3354.03	29.61	1.62×10^{-10}
7	46.398	0.99991	3141.85	29.79	30.19×10^{-10}
8	46.497	0.99983	3143.91	39.71	22.33×10^{-10}

Abbreviation: LC_{50}, lethal concentration.

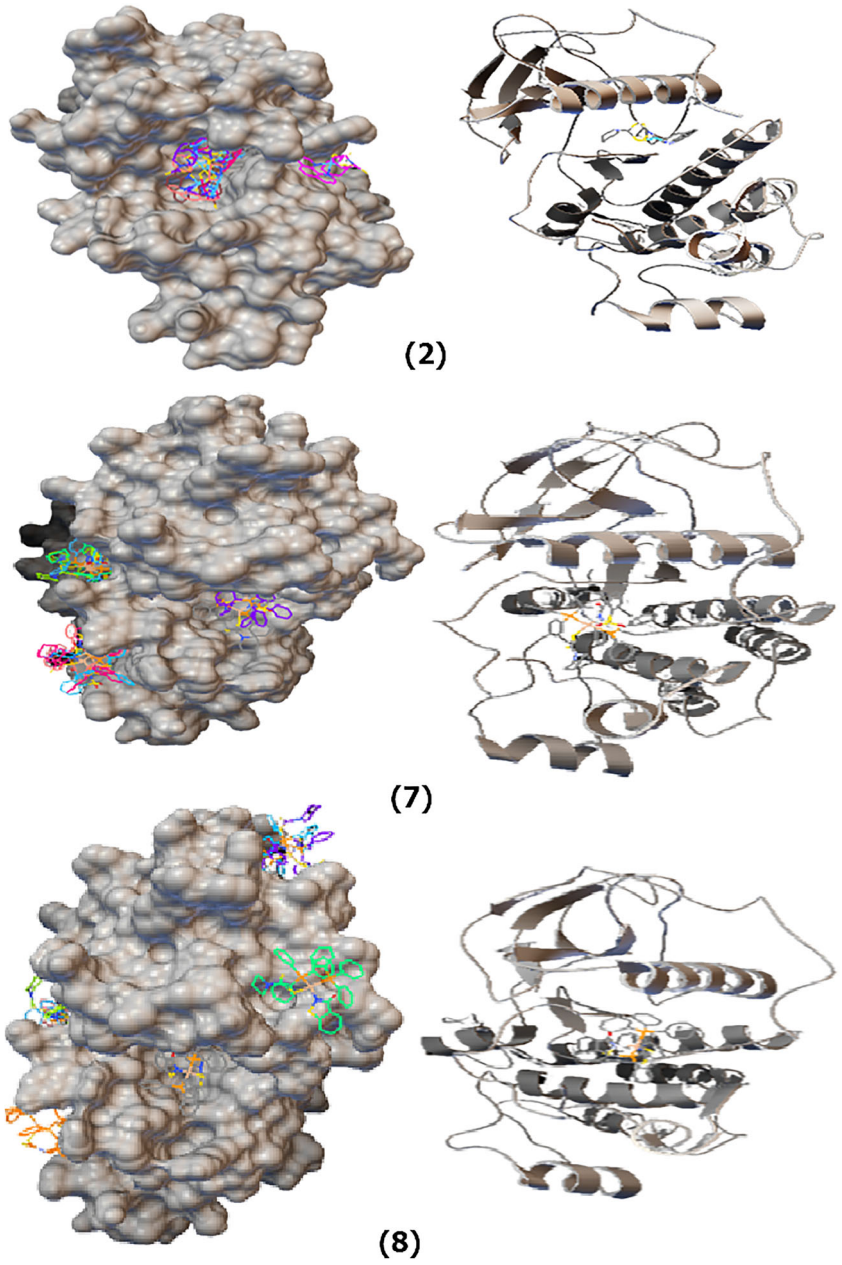

FIGURE 4 Molecular interactions between complexes **2**, **7**, and **8** with receptor

TABLE 5 Binding energy values and ligand efficiency of the studied complexes

Comp.	E_b (kcak/mol)	L_E	E_b (kcak/mol) range	Best site number
[Zn(κ^2-PipDT)$_2$]	−7.65	−0.20	−6.05 to −7.65	3
[Pd(κ^2-PipDT)$_2$]	−5.47	−0.27	−5.11 to −5.47	3
1	−6.30	−0.20	−4.10 to −6.3	4
2	−8.68	−0.26	−3.35 to −8.68	7
3	−5.36	−0.16	−1.91 to −5.36	5
4	−7.83	−0.25	−4.54 to −7.83	5
5	−6.54	−0.20	−3.98 to −6.54	6
6	−5.13	−0.16	−2.26 to −5.13	4
7	−4.74	−0.08	−1.98 to −4.74	9
8	−6.25	−0.10	−1.69 to −6.25	4

2 (VEGFRTK) (3wze).[75] The potency interaction of the [Zn(κ^2-PipDT)$_2$], [Pd(κ^2-PipDT)$_2$], and (**1–8**) complexes with receptor depending on binding energy and ligand efficiency. The measure of the affinity of complexes and the receptor is a binding energy (E_b) and ligand efficiency (L_E) is binding energy per atom of ligand to receptor protein.[49] The best location in receptor in depending on E_b for all complexes as and the range of E_b for the complexes in different sites as present in Table 5. The order of the ability to block the protein structure by the E_b is

$$\mathbf{2} > \mathbf{4} > \left[\mathrm{Zn}\left(\kappa^2-\mathrm{PipDT}\right)_2\right] > \mathbf{5} > \mathbf{1} > \mathbf{7} > \left[\mathrm{Pd}\left(\kappa^2-\mathrm{PipDT}\right)_2\right] > \mathbf{3} > \mathbf{6} > \mathbf{8}.$$

Therefore, it shall be given high precedence for complexes **2**, **4**, [Zn(κ^2-PipDT)$_2$], **5**, and **1** while the other could take low importance. High, median, and low inhibition complexes are **2**, **7**, and **8**, respectively, shown in Figure 5, and the other includes in Figure S3.

4 | CONCLUSION

We synthesized eight mixed ligand complexes of Zn (II) and Pd (II) complexes by the reaction of [M(κ^2-PipDT)$_2$] {M═Zn or Pd} complex with amine ligands (2,2 bipyridyl, 1,10-phenanthroline, and 3-aminopyridine) or reaction of *cis*-[$PdCl_2(PPh_3)_2$] with sodium benzisothiazolinate (Nabit) or sodium saccharinate (Nasac), followed by addition, sodium piperidine dithiocarbamate. In addition, the complexes were characterized by elemental analysis and spectroscopic techniques (IR, ^{1}H, ^{31}P-{1H} NMR,. The PipDT anion was coordinated as monodentate fashion through the sulfur atom to afford a tetrahedral shape around the Zn (II) and square planner around the Pd (II) center. The complexes evaluating the antimicrobial properties and the antimicrobial activities of the complexes were in the order of {**8** > **7** > **3** > **6** > **4** > **1** > **NaPipDT**}. Furthermore, theoretical part presented the oxygen atom in zinc complexes has a high electron density by TED and ESP maps but the palladium atom in other. Also, high concentrations could use in human body according to LC_{50} predicted values. While the Autodock study explains the ability of use complexes as anticancer and the good, inhibitions are **2**, **4**, **[Zn(κ^2-PipDT)$_2$]**, **5**, and **1**.

AUTHOR CONTRIBUTIONS

Ahmed Al-Janabi: Investigation; supervision. **Mustafa Kadhim:** Methodology; software. **Amenah Al-Nassiry:** Formal analysis; investigation; methodology. **Tarek Yousef:** Formal analysis; investigation; software.

ORCID

Ahmed S.M. Al-Janabi https://orcid.org/0000-0003-2722-7419
Tarek A. Yousef https://orcid.org/0000-0003-3039-7646

REFERENCES

[1] G. Hogarth, *Mini-Rev. Med. Chem.* **2012**, *12*, 1202. https://doi.org/10.2174/138955712802762095
[2] M. K. Amir, S. Z. Khan, F. Hayat, A. Hassan, I. S. Butler, *Inorg. Chim. Acta* **2016**, *451*, 31. https://doi.org/10.1016/j.ica.2016.06.036
[3] A. T. Odularu, P. A. Ajibade, *Bioinorg. Chem. Appl.* **2019**, *2019*, 1. https://doi.org/10.1155/2019/8260496
[4] J. W. de, F. Oliveira, H. A. O. Rocha, W. M. T. Q. de Medeiros, M. S. Silva, *Molecules* **2019**, *24*, 2806. https://doi.org/10.3390/molecules24152806
[5] I. Haiduc, *Compr. Coord. Chem. II.* **2004**, *1*, 349. https://doi.org/10.1016/B0-08-043748-6/01121-X
[6] P. J. Heard, Main group dithiocarbamate complexes, in *Progress in Inorganic Chemistry*, (Ed: K. D. Karlin) Vol. 53, John Wiley & Sons, Inc, Hoboken, New Jersey **2005** 1.
[7] G. Hogarth, Transition metal dithiocarbamates: 1978–2003, in *Progress in Inorganic Chemistry*, (Ed: K. D. Karlin) Vol. 53, John Wiley & Sons, Inc **2005** 71. https://onlinelibrary.wiley.com/doi/abs/10.1002/0471725587.ch2
[8] S. Kanchi, P. Singh, K. Bisetty, *Arab. J. Chem.* **2014**, *7*, 11. https://doi.org/10.1016/j.arabjc.2013.04.026
[9] C. L. Donnici, L. J. Nogueira, M. H. Araujo, S. R. Oliveira, T. F. F. Magalhães, M. T. P. Lopes, A. C. A. Silva, A. M. Da Costa Ferreira, C. V. B. Martins, M. A. De Resende Stoianoff, *Molecules* **2014**, *19*, 5402. https://doi.org/10.3390/molecules19045402
[10] F. K. Keter, I. A. Guzei, M. Nell, W. E. V. Zyl, J. Darkwa, *Inorg. Chem.* **2014**, *53*, 2058. https://doi.org/10.1021/ic4025926
[11] N. Shimar, Z. Goh, Y. Kqueen, K. Ang, J. Horng, C. Hoon, Z. Abidin, S. Nadiah, B. Abdul, S. Weng, H. Seng, E. R. T. Tiekink, *Eur. J. Med. Chem.* **2013**, *67*, 127. https://doi.org/10.1016/j.ejmech.2013.06.038
[12] E. J. Ferna, M. Lo, M. Monge, E. Olmos, A. Laguna, E. Zaragoza, P. G. Jones, *Inorg. Chem.* **1998**, *37*, 5532.
[13] C. S. Lai, E. R. T. Tiekink, *Appl. Organmetal. Chem.* **2003**, *17*, 143. https://doi.org/10.1002/aoc.383
[14] J. W. Faamau, E. R. T. Tiekink, *J. Coord. Chem.* **1994**, *31*(2), 93. https://doi.org/10.1080/00958979408024204
[15] E. P. Cullen, J. Doherty, A. R. Manning, P. Mcardle, D. Cunningham, *J. Org. Chem.* **1988**, *348*, 109.
[16] P. J. Rani, S. Thirumaran, *Eur. J. Med. Chem.* **2013**, *62*, 139. https://doi.org/10.1016/j.ejmech.2012.12.047
[17] A. I. A. Al-Nassiry, A. S. M. Al-Janabi, O. Y. T. Al-Janabi, P. Spearman, M. A. Al-Heety, *J. Chin. Chem. Soc.* **2020**, *67*, 775. https://doi.org/10.1002/jccs.201900349
[18] S. Hosseinzadeh, M. E. Moghadam, S. Sheshmani, A. S. Shahvelayati, *J. Biomol. Struct. Dyn.* **2019**, *38*(8), 2215. https://doi.org/10.1080/07391102.2019.1627909

[19] L. D. Nyamen, A. A. Nejo, V. S. R. Pullabhotla, P. T. Ndifon, M. Azad, J. Akhtar, P. O. Brien, N. Revaprasadu, *Polyhedron* **2014**, *67*, 129. https://doi.org/10.1016/j.poly.2013.08.061

[20] E. Sathiyaraj, M. Venkatesh, *J. Saudi Chem. Soc.* **2018**, *22*, 527. https://doi.org/10.1016/j.jscs.2017.09.002

[21] H. Khan, A. Badshah, M. Said, G. Murtaza, J. Ahmad, B. J. Jean-claude, M. Todorova, I. S. Butler, *Appl. Organomet. Chem.* **2013**, *27*, 387. https://doi.org/10.1002/aoc.2991

[22] E. Sathiyaraj, S. Thirumaran, *Spectrochim. Acta Part a Mol. Biomol. Spectrosc.* **2012**, *97*, 575. https://doi.org/10.1016/j.saa.2012.06.052

[23] D. C. Onwudiwe, C. A. Strydom, E. C. Hosten, *Inorg. Chim. Acta* **2013**, *401*, 1. https://doi.org/10.1016/j.ica.2013.03.010

[24] J. Adeyemi, D. Onwudiwe, *Molecules* **2020**, *25*, 305. https://doi.org/10.3390/molecules25020305

[25] P. Taylor, M. I. Moghaddam, A. Divsalar, *J. Biomol. Struct. Dyn.* **2009**, *26*(5), 575. https://doi.org/10.1080/07391102.2009.10507273

[26] D. C. Onwudiwe, P. A. Ajibade, *Int. J. Mol. Sci.* **2011**, *12*, 1964. https://doi.org/10.3390/ijms12031964

[27] G. Faraglia, D. Fregona, S. Sitran, L. Giovagnini, C. Marzano, F. Baccichetti, U. Casellato, R. Graziani, *J. Inorg. Biochem.* **2001**, *83*, 31.

[28] S. Hussain, S. Thirumaran, S. Selvanayagam, *Polyhedron* **2015**, *96*, 16. https://doi.org/10.1016/j.poly.2015.04.020

[29] A. C. Ekennia, D. C. Onwudiwe, C. Ume, E. E. Ebenso, *Bioinorg. Chem. Appl.* **2015**, *2015*, 1. https://doi.org/10.1155/2015/913424

[30] P. A. Ajibade, D. C. Onwudiwe, *J. Coord. Chem.* **2015**, *64*(17), 2963. https://doi.org/10.1080/00958972.2011.606906

[31] S. I. Islam, S. B. Das, S. Chakrabarty, S. Hazra, A. Pandey, A. Patra, *Adv. Chemother.* **2016**, *2016*, 1. https://doi.org/10.1155/2016/4676524

[32] H. Mansouri-torshizi, M. Saeidifar, F. Khosravi, A. Divsalar, A. A. Saboury, F. Hassani, *Bioinorg. Chem. Appl.* **2015**, *2011*, 1. https://doi.org/10.1155/2011/394506

[33] S. Z. Khan, I. S. Butler, F. Bélanger-Gariepy, *Inorg. Chem. Commun.* **2019**, *105*, 140. https://doi.org/10.1016/j.inoche.2019.04.019

[34] B. A. Prakasam, M. Lahtinen, A. Peuronen, M. Muruganandham, E. Kolehmainen, E. Haapaniemi, M. Sillanpaa, *J. Mol. Struct.* **2016**, *1108*, 195. https://doi.org/10.1016/j.molstruc.2015.11.076

[35] L. Marchesellil, C. Pretil, M. Tagliazucchil, V. Cherchiz, L. Sindellari, A. Furlani, A. Papaioannou, V. Scarcia, *Eur. J. Med. Chem.* **1993**, *28*, 347.

[36] M. Shahid, T. Rüffer, H. Lang, A. Awan, S. Ahmad, *J. Coord. Chem.* **2009**, *63*(2), 440. https://doi.org/10.1080/00958970802255741

[37] D. C. Onwudiwe, P. A. Ajibade, *Polyhedron* **2010**, *29*, 1431. https://doi.org/10.1016/j.poly.2010.01.011

[38] F. P. Andrew, P. A. Ajibade, *J. Mol. Struct.* **2017**, *1155*, 843. https://doi.org/10.1016/j.molstruc.2017.10.106

[39] M. B. Hursthouse, M. A. Malik, M. Motevalli, P. O. Brien, *Organometallic* **1991**, *2*, 730.

[40] S. H. Abbas, *Eur. J. Chem.* **2017**, *8*(4), 367. https://doi.org/10.5155/eurjchem.8.4.367-370.1636

[41] A. S. M. Al-Janabi, O. A. Y. Al-Samrai, T. A. Yousef, *Appl. Organomet. Chem.* **2020**, *34*, e5967. https://doi.org/10.1002/aoc.5967

[42] A. S. M. Al-Janabi, O. A. Y. Al-Samrai, E. A. Othman, T. A. Yousef, *Appl. Organomet. Chem.* **2020**, *34*. https://doi.org/10.1002/aoc.5996

[43] M. M. Salman, A. A. Al-Dulaimi, A. S. M. Al-Janabi, M. A. Al-Heety, *Mater. Today: Proc.* **2020**. https://doi.org/10.1016/j.matpr.2020.07.082

[44] (a)M. Bardaji, N. G. Connelly, M. C. Gimeno, J. Jimeneza, P. G. Jones, A. L. A. M. Lagunaa, *J. Chem. Soc. Dalton Trans.* **1994**, *867*, 1163. (b)F. Conan, J. S. Pala, M. Garland, R. Baggio, *Inorg. Chim. Acta* **2008**, *278*, 108.

[45] (a)M. Sokolov, H. Imoto, T. Saito, *Inorg. Chem. Comm.* **1999**, *2*, 422. (b) A. W. Salman, G. U. Rehman, N. Abdullah, S. Budagumpi, S. Endud, H. H. Abdallah, *Inorg. Chim. Acta* **2015**, *438*, 14. https://doi.org/10.1016/j.ica.2015.08.027

[46] K. Sayin, S. E. Kariper, M. Taştan, T. A. Sayin, D. Karakaş, *J. Mol. Struct.* **2019**, *1176*, 478. https://doi.org/10.1016/j.molstruc.2018.08.103

[47] E. A. Hussein, I. M. Shaheed, R. S. Hatam, M. M. Kadhim, D. T. Al-kadhum, *Sys. Rev. Pharm.* **2020**, *11*, 495. https://doi.org/10.5530/srp.2020.3.63

[48] M. Wojciechowski, *J. Mol. Graphics Modell.* **2017**, *78*, 74. https://doi.org/10.1016/j.jmgm.2017.09.016

[49] H. Li, K. S. Leung, P. J. Ballester, M. H. Wong, *PLoS ONE* **2014**, *9*, e85678. https://doi.org/10.1371/journal.pone.0085678

[50] R. A. Saleh, H. A. Mohammad, T. I. Gerber, E. C. Hosten, *AIP Conf. Proc.* **2017**, *1888*, 020047. https://doi.org/10.1063/1.5004324

[51] A. W. Bauer, *Arch. Intern. Med.* **1959**, *104*(2), 208.

[52] H. M. Berman, *Nucleic Acids Res.* **2000**, *28*, 235. https://doi.org/10.1093/nar/28.1.235

[53] A. Allouche, *J. Comput. Chem.* **2012**, *32*, 174. https://doi.org/10.1002/jcc

[54] D. R. Koes, M. P. Baumgartner, C. J. Camacho, *J. Chem. Inf. Model.* **2013**, *53*, 1893. https://doi.org/10.1021/ci300604z

[55] Æ. Frisch, R. E. Plata, D. A. Singleton, *J. Am. Chem. Soc.* **2009**, *137*, 3811. https://doi.org/10.1021/ja5111392

[56] E. A. Yaqo, R. A. Anaee, M. H. Abdulmajeed, I. H. R. Tomi, M. M. Kadhim, *Chem. Pap.* **2020**, *74*, 1739. https://doi.org/10.1007/s11696-019-01022-2

[57] A. S. Al-Janabi, A. A. Al-Dulaimi, H. M. Gergees, M. H. Saleh, *Orient. J. Chem.* **2019**, *35*(1), 186. https://doi.org/10.13005/ojc/350121

[58] M. K. Yadav, G. Rajput, A. N. Gupta, V. Kumar, M. G. B. Drew, N. Singh, *Inorg. Chim. Acta* **2014**, *421*, 210. https://doi.org/10.1016/j.ica.2014.05.031

[59] K. Nakamoto, *Infra-Red and Raman Spectra of Inorganic and Coordination Compounds*, 4th ed., John Wiley & Sons, New York **1986**.

[60] F. X. Silverstein, R. M. Webster, *Spectrometric Identification of Organic Compounds*, 6th ed., John Wiley & Sons, New York **1997**.

[61] S. A. Al-Jibori, W. J. Hameed, A. S. Al-Janabi, S. Basak-modi, C. Wagner, G. Hogarth, *Inorg. Chim. Acta* **2018**, *479*, 197. https://doi.org/10.1016/j.ica.2018.04.050

[62] M. H. S. Al-jibori, N. H. Buttrus, A. S. M. Al-Janabi, *J. Pure Sci.* **2017**, *22*(2), 99.

[63] S. A. Al-Jibori, A. R. Al-Jibori, H. A. Mohamad, A. S. Al-Janabi, C. Wagner, G. Hogarth, *Inorg. Chim. Acta* **2019**, *488*, 152. https://doi.org/10.1016/j.ica.2019.01.017
[64] D. C. Onwudiwe, Y. Boitumelo, A. C. Ekennia, E. Hosten, *Inorg. Chim. Acta* **2016**, *447*, 134. https://doi.org/10.1016/j.ica.2016.03.033
[65] R. S. Joseyphus, M. S. Nair, *Mycobiology* **2008**, *36*, 93.
[66] N. Raman, J. Joseph, A. S. K. Velan, C. Pothiraj, *Mycobiology* **2006**, *34*, 214.
[67] R. Sato, S. Vohra, S. Yamamoto, K. Suzuki, K. Pavel, S. Shulga, Y. Blume, N. Kurita, *J. Mol. Graphics Modell.* **2020**, *98*, 107611.
[68] D. Majumdar, D. K. Singh, D. K. Pandey, D. Parai, K. Bankura, D. Mishra, *J. Mol. Struct.* **2020**, *1209*, 127936.
[69] M. S. Almutairi, D. Leenaraj, H. A. Ghabbour, I. H. Joe, M. I. Attia, *J. Mol. Struct.* **2019**, *1180*, 110.
[70] T. A. Yousef, *J. Mol.Struct.* **2020**, *1215*, 128180.
[71] T. A. Yousef, G. M. A. El-Reash, R. M. El Morshedy, *Polyhedron* **2012**, *45*, 71.
[72] T. A. Yousef, O. K. Alduaij, G. M. Abu El-Reash, R. M. El Morshedy, *J. Mol. Liq.* **2016**, *222*, 762.
[73] E. A. Yaqo, R. A. Anaee, M. H. Abdulmajeed, I. H. R. Tomi, M. M. Kadhim, *ChemistrySelect* **2019**, *4*, 9883. https://doi.org/10.1002/slct.201902398
[74] E. Eroglu, S. Palaz, O. Oltulu, H. Turkmen, C. Ozaydin, *Int. J. Mol. Sci.* **2007**, *8*, 1265. https://doi.org/10.3390/ijms8121265
[75] A. W. Salman, G. Ur Rehman, N. Abdullah, S. Budagumpi, S. Endud, H. Hadi Abdallah, W. Y. Wong, *Polyhedron* **2014**, *81*, 499. https://doi.org/10.1016/j.poly.2014.06.054

SUPPORTING INFORMATION

Additional supporting information may be found online in the Supporting Information section at the end of this article.

How to cite this article: Al-Janabi ASM, Kadhim MM, Al-Nassiry AIA, Yousef TA. Antimicrobial, computational, and molecular docking studies of Zn (II) and Pd (II) complexes derived from piperidine dithiocarbamate. *Appl Organomet Chem*. 2020;e6108. https://doi.org/10.1002/aoc.6108